Inorg. Chem. **2007**, *46*, 2471–2477

Structural and Magnetic Properties of MCl_2 (M = Fe, Mn, Co): Acetonitrile Solvates

Konstantin I. Pokhodnya,[#] Michael Bonner,[#] Antonio G. DiPasquale,[§] Arnold L. Rheingold,[§] Jae-Hyuk Her,[†] Peter W. Stephens,[†] Jong-Won Park,[#] Bretni S. Kennon,[#] Atta M. Arif,[#] and Joel S. Miller*[,#]

Department of Chemistry, 315 S. 1400 E. RM 2124, University of Utah, Salt Lake City, Utah 84112-0850, Department of Chemistry and Biochemistry, University of California, San Diego, La Jolla, California 92093-0358, Department of Physics and Astronomy, Stony Brook University, Stony Brook, New York 11794-3800

Received September 29, 2006

$M^{II}Cl_2$ (M = Mn, Fe, Co) as their acetonitrile solvates were isolated, and their structural, spectroscopic, and magnetic properties were studied. $MCl_2(NCMe)_2$ (M = Fe, Mn) form 1-D chains of octahedral M^{II} ions with four bridging chlorides and two axial MeCN's. The presence of an axial distortion for MFe causes a significant magnetic anisotropy that increases significantly below 150 K; however, χ_{av} [$=(\chi_{II} + 2\chi_{\perp})/3$] almost coincides with the value obtained on a polycrystalline sample. $MnCl_2(NCMe)_2$ is a paramagnet with a weak antiferromagnetic coupling. Annealing $FeCl_2(NCMe)_2$ at 55 °C forms the monosolvate of $FeCl_2(NCMe)$ composition in which two chains collapse into a double chain with formation of Fe–Cl bonding such that half of the μ-Cl's becomes μ_3-Cl's. This material orders magnetically below T_c = 4.3 K. For M = Co, paramagnetic tetrahedral $[CoCl_3(NCMe)]^-$ anions are isolated.

Introduction

Molecule-based magnets are a relatively new class of magnetic materials in which inorganic and/or organic ions or molecules bearing unpaired electron spin density strongly interact magnetically through bonds and/or space.[1] $M^{II}[TCNE]_x$ (MV, Mn, Fe, Co, Ni; TCNE tetracyanoethylene; $x \approx 2$) organic-based magnets have magnetic ordering temperatures, T_c, that range from 44 (M = Co, Ni)[2] up to ~400 K for M = V.[3]

$M^{II}[TCNE]_2$ (MFe, Mn, Co, Ni) magnets can be prepared from the reaction of the corresponding anhydrous M(II) iodide, which was used in the form of the MeCN solvate, and TCNE in CH_2Cl_2 solution.[2] However, albeit a priority, the elucidation of the structures of $M[TCNE]_2$ (M = Mn, Fe) has been elusive.

Thus, to optimize and finely tune the structural and magnetic properties of the $M[TCNE]_2$ magnets, as well as to fabricate new magnets with different composition, the synthesis and detailed study of the M(II) halides precursors is important. For example, the reaction of the acetonitrile solvate of $FeCl_2$, $FeCl_2(NCMe)_2$, with TCNE forms a new family of organic-based magnets of $Fe_2Cl_4(NCMe)_2(TCNE)$ composition.[4] Hence, herein we report the structural, spectroscopic, and magnetic characterization of MCl_2 (MMn, Fe, Co), as their acetonitrile solvates of $FeCl_2(NCMe)_2$, $FeCl_2(NCMe)$, $MnCl_2(NCMe)_2$, and $[Co^{II}Cl_3(NCMe)]^-$ composition.

Experimental Section

All manipulations were performed under an inert nitrogen atmosphere (<1 ppm O_2 and <1 ppm H_2O) using Vacuum Atmospheres DriLab glove boxes. All solvents were sparged with

* To whom correspondence should be addressed. E-mail: jsmiller@chem.utah.edu.
[#] University of Utah.
[§] University of California.
[†] Stony Brook University.

(1) Recent reviews: Ovcharenko, V. I.; Sagdeev, R. Z. Russ. *Chem. Rev.* **1999**, *68*, 345. Kinoshita, M. *Phil. Trans. R. Soc. Lond. A* **1999**, *357*, 2855. Miller, J. S.; Epstein, A. J. *Chem. Commun.* **1998**, 1319. Miller, J. S.; Epstein, A. J. *Chem. Eng. News* **1995**, *73* (40), 30.
(2) Zhang, J.; Ensling, J; Ksenofontov, V.; Gütlich, P.; Epstein, A. J.; Miller, J. S. *Angew. Chem., Int. Ed.* **1998**, *37*, 657. Miller, J. S. Unpublished result.
(3) (a) Manriquez, J. M; Yee, G. T.; McLean, R. S.; Epstein, A. J.; Miller, J. S. *Science* **1991**, *252*, 1415. (b) Miller, J. S.; Yee, G. T.; Manriquez, J. M.; Epstein, A. J. In *Proceedings of Nobel Symposium #NS-81 Conjugated Polymers and Related Materials: The Interconnection of Chemical and Electronic Structure*; Oxford University Press: New York, 1993; p 461; *La Chim. La Ind.* **1992**, *74*, 845. (c) Zhang, J.; Zhou, P.; Brinckerhoff, W.B.; Epstein, A. J.; Vazquez, C.; McLean, R. S.; Miller, J. S. A. C. S. *Sym. Ser*. **1996**, *644*, 311.
(4) Pokhodnya, K. I.; Bonner, M.; Her, J.-H.; Stephens, P. W.; Miller, J. S. Submitted for publication.

10.1021/ic061877n CCC: $37.00
Published on Web 03/06/2007

nitrogen and passed over two columns of activated alumina prior to use to remove traces of oxygen and water.[5] Anhydrous iron, manganese, and cobalt(II) chlorides were used without additional purification as purchased. The CryoLoop and Paratone-N oil were obtained from Hampton Research.

$FeCl_2(NCMe)_2$ (1). Anhydrous $Fe^{II}Cl_2$ (2.00 g; 15.8 mmol) was dissolved in ~100 mL of MeCN. The mixture was refluxed overnight. The solution was cooled to room temperature and filtered twice using fine fritted glass. The solution was warmed to ~50 °C, and its volume was reduced to ~5 mL. Upon addition of ~100 mL of Et_2O a white fine powder precipitated, which was isolated by filtration, washed with Et_2O, and dried in the glove box atmosphere (Yield: 2.2 g; 67%) of $Fe^{II}Cl_2(NCMe)_2$. IR (KBr, cm^{-1}): 2992 m, 2933 s, 2310 m, 2282 s, 1421 br, 1378 m, 1030 br, 938 m, 788 m, 471 w. Colorless prism-shaped crystals up to $5 \times 1 \times 0.5$ mm^3 in size were grown by slow Et_2O vapor diffusion into saturated MeCN solution at room temperature.

$FeCl_2(NCMe)$ (1a). 1a was prepared by annealing polycrystalline **1** at 55 ± 5 °C for 2 h in nitrogen atmosphere, and a 17.0% weight loss occurred suggesting $FeCl_2(NCMe)_{1.13}$. The observed (calcd[6]) elemental analysis for $FeCl_2(NCMe)_{0.9}$ is %C = 13.09 (13.21), %H = 1.65 (2.04), %N = 7.42 (7.70). This deviates from the expected $x = 1.13$ value and reflects that **1** easily loses MeCN even at ambient conditions. Attempts to obtain **1a** with $x \approx 1$ by changing the annealing time and/or temperature led to materials with admixture of **1** or poorer crystallinity (weaker and broader XRD peaks). IR (KBr, cm^{-1}): 3002 m, 2939 s, 2310 s, 2283 s, 1442 m, 1431 m, 1418 m, 1405 m, 1368 m, 1031 m, 938 m, 788 m, 471 w. This composition was confirmed via the determination of the structure of **1a**.

$MnCl_2(NCMe)_2$ (2). Anhydrous $Mn^{II}Cl_2$ (1.00 g; 7.9 mmol) was added to ~200 mL of MeCN, and the turbid solution was refluxed over 4 days. The remaining pink powder was filtered, washed with 50 mL of MeCN, and dried under vacuum (Yield: 1.630 g; 98%). Cottonlike pink crystals were obtained by recrystallization from hot MeCN. Needle-shaped pink crystals were grown by slow cooling of the saturated MeCN solution. IR(KBr, cm^{-1}): 2994 m, 2933 s, 2309 m, 2280 s, 1422 br, 1378 m, 1030 br, 936 m, 781 m, 470 w.

$[Co^{II}(NCMe)_6][Co^{II}Cl_3(NCMe)]_2 \cdot MeCN$ (3). Anhydrous $Co^{II}Cl_2$ (1.00 g; 7.7 mM) was dissolved in 50 mL of MeCN and heated to reflux for 2 h. The solution was cooled down to room temperature and filtered two times using fine fritted glass. The solution was warmed to ~50 °C, and its volume was reduced to ~5 mL. Upon addition of ~100 mL of Et_2O a blue powder precipitated, which was isolated by filtration, washed with Et_2O, and dried in the glove box atmosphere (Yield: 1.42 g; 69%) of $[Co^{II}(NCMe)_6][Co^{II}Cl_3(NCMe)]_2 \cdot MeCN$. IR(KBr, cm^{-1}): 2990 m, 2927 s, 2315 s, 2284 s, 1410 m, 1366 m, 1034 s, 940 m, 791 m. Dark blue prism-shaped crystals up to $10 \times 1 \times 0.5$ mm^3 in size were grown by slow Et_2O vapor diffusion into saturated MeCN solution at room temperature.

Physical Properties. The thermal properties were studied on a TA Instruments Model 2050 thermogravimetric analyzer (TGA) equipped with a TA-MS Fison triple-filter quadrupole mass spectrometer to identify gaseous products with masses less than 300 amu. This instrument was located in a Vacuum Atmospheres DriLab box under nitrogen to protect air- and moisture-sensitive samples. Samples were placed in an aluminum pan and heated at 5 °C/min under a continuous 10-mL/min nitrogen flow. A TA Instruments Model 2910 analyzer instrument was used to carry out differential scanning calorimetry (DSC) experiments. Samples were loaded into an aluminum pan with a lid and sealed airtight with a special press inside the box; they were transferred into the instrument on air, and DSC experiments were performed under nitrogen gas flow.

The 2−300-K magnetic susceptibility was determined on a Quantum Design MPMS-5XL 5 T SQUID or a 9 T PPMS susceptometer as previously described.[7] In addition to correcting for the diamagnetic contribution from the sample holder, core diamagnetic corrections based on summing Pascal's constants were used. Infrared spectra (50−4000 cm^{-1}; 1 cm^{-1} resolution) were obtained on a Bruker Tensor 37 FT spectrophotometer as KBr pellets or Nujol mulls.

X-ray powder diffraction (XRD) scans were obtained on a θ/θ Bruker AXS D8 Advance diffractometer (2θ of 5−50° step width of 0.01° counting time of 20 s/step, voltage of 40 kV, and current of 40 mA). The X-ray beam was filtered with a Göbel mirror to remove all but the Cu $K_{\alpha 1}$ radiation ($\lambda = 1.54060$ Å). Samples were sealed under inert atmosphere in 1.0-mm thin-walled quartz capillaries to prevent oxidation, and scans were performed at room temperature (~298 K). Additional powder diffraction measurements for Rietveld structure analysis are as described below.

X-ray Crystallography. Structure of 1. A single crystal of **1** ($0.35 \times 0.33 \times 0.30$ mm^3) was mounted on a glass fiber with traces of viscous oil and then transferred to a Nonius Kappa CCD diffractometer equipped with Mo K_α radiation ($\lambda = 0.71073$ Å). Ten frames of data were collected at 150(1) K with an oscillation range of 1°/frame and an exposure of 20 s/frame. The structure was solved by a combination of direct methods and heavy atom using SIR 97.[8] All of the non-hydrogen atoms were refined with anisotropic displacement coefficients. Hydrogen atoms were assigned isotropic displacement coefficients $U(H) = 1.5U(C_{methyl})$, and their coordinates were allowed to ride on their respective carbons using SHELXL97.[9] The asymmetric unit contains two independent molecules. The weighting scheme employed was $w = 1/[\sigma^2(F_o^2) + (0.045P)^2 + 4.8534P]$ where $P = (F_o^2 + 2F_c^2)/3$. A summary of data collection parameters for compounds **1** and **2** is given in Table 1.

Structure of 1a. A white powder of **1a** was sealed in a thin-wall quartz capillary in an inert atmosphere, and a high-resolution powder diffraction pattern was collected at X16C beamline of the National Synchrotron Light Source, Brookhaven National Laboratory. A Si(111) channel-cut monochromator selected a 0.6908(2)-Å highly parallel incident beam. The diffracted X-rays were analyzed by a Ge(111) single-reflection crystal and detected using a NaI scintillation counter. All measurements were done at ambient temperature, and the capillary was rotated during data collection for better averaging.

The TOPAS-Academic program was used to index, solve, and refine the crystal structure.[10−12] The space group $P2_1/n$ (No. 14)

(5) Pangborn, A. B.; Giardello, M. A.; Grubbs, R. H.; Rosen, R. K.; Timmers, F. J. *Organometallics* **1996**, *15*, 1518.
(6) Miller, J. S.; Kravitz, S. H; Kirschner, S.; Ostrowski, P.; Nigrey, P. J. *J. Chem. Ed*. **1977**, *55*, 181; *Quant. Chem. Prog. Exch*. **1977**, *10*, 341.
(7) Brandon, E. J.;Rittenberg, D. K.; Arif, A. M.; Miller, J. S. *Inorg. Chem.* **1998**, *37*, 3376.
(8) Altomare, A.; Burla, M. C.; Camalli, M.; Cascarano, G.; Giacovazzo, C.; Guagliardi, A.; Moliteni, A. G. G.; Polidori, G.; Spagna, R. *SIR97 (Release 1.02) - A program for automatic solution and refinement of crystal structure*; Instituto di Ricera per lo Svilupppo di Metodologie Cristallografiche: Bari, Italy, 1997
(9) Sheldrick, G. M. *SHELX97 [Includes SHELXS97, SHELXL97, CIFTAB)−Programs for Crystal Structure Analysis (Release 97-2.)*; University of Göttingen: Göttingen, Germany, 1997.
(10) *TOPAS V3: General profile and structure analysis software for powder diffraction data−User's Manual*; Bruker AXS: Karlsruhe, Germany, 2005.
(11) Coelho, A. A. *J. Appl. Crystallogr*. **2000**, *33*, 899

Table 1. Summary of Crystallographic Data for $MCl_2(NCMe)_2$ [M = Fe (**1**), Mn(**2**)], $MCl_2(NCMe)$ (**1a**), and $[NEt_4][Co^{II}Cl_3(NCMe)]$ (**4**)

compound	$FeCl_2(NCMe)_2$ (**1**)	$FeCl_2(NCMe)$ (**1a**)	$MnCl_2(NCMe)_2$ (**2**)	$[NEt_4][Co^{II}Cl_3(NCMe)]$ (**4**)
cryst syst	orthorhombic	monoclinic	orthorhombic	monoclinic
formula	$C_4H_6Cl_2FeN_2$	$C_2H_3Cl_2FeN$	$C_4H_6Cl_2MnN_2$	$C_{10}H_{23}Cl_3CoN_2$
fw	208.86	167.81	207.95	336.60
space group	*Pbam*	$P2_1/n$	*Pbam*	*Pn*
a, Å	8.0558(3)	18.2005(10)	8.125(3)	7.2674 (5)
b, Å	13.3799(4)	8.3809(4)	13.368(5)	13.2740 (9)
c, Å	3.7029(1)	3.6573(2)	3.7430(15)	8.2674 (5)
β, deg	90.00	94.167(3)	90.00	90.02(1)
Z	2	4	2	2
T, K	150(1)	295	100(2)	100(2)
V, Å^3	399.12(2)	556.39(10)	406.6(3)	797.53(9)
ρ_{calcd}, g/cm^3	1.738	2.003	1.699	1.402
R1[a]	0.0167	0.0449	0.0228	0.0443
wR2[b]	0.0415	0.0516	0.0592	0.1145
GOF on F^2 [c]	1.125	1.715	1.167	1.015

[a] $R1 = \sum||F_o| - |F_c||/\sum|F_o|$. [b] $wR2 = [\sum(w(F_o^2 - F_c^2)^2)/\sum(F_o^2)^2]^{1/2}$. [c] $F^2 = [\sum(w(F_o^2 - F_c^2)^2/(n - p)\ ]^{1/2}$.

was hypothesized by checking the systematic absences of Pawley whole pattern fits. The simulated annealing method implemented in TOPAS was used to solve the structure, producing the structure discussed below. After obtaining an acceptable agreement between observed and calculated XRPD patterns from the structure solution, Rietveld refinements were performed to improve the fits and determine atomic positions. Only four independent isotropic thermal factors were used. Fe, each Cl, and all atoms in acetonitrile.

Structure of 2. A colorless needle 0.20 × 0.07 × 0.03 mm^3 in size was mounted on a CryoLoop with Paratone oil. The crystal-to-detector distance was 60 mm, and the exposure time was 10 s/frame using a scan width of 0.3° Data collection was 100% complete up to 25° in θ. A total of 3224 reflections was collected covering the indices, $h = -10$ to 10, $k = -17$ to 17, and $l = -4$ to 4. The number of reflections that were found to be symmetry independent was 555, with an R_{int} of 0.0234, indicating that the data were of excellent quality (average = 0.07). Indexing and unit cell refinement indicated a primitive, orthorhombic lattice. The space group was found to be *Pbam* (No. 55). The data were integrated using the Bruker SAINT software program and corrected for absorption using the Bruker SADABS software program. Solution by direct methods (SIR-2004) produced a complete heavy-atom phasing model consistent with the proposed structure. All non-hydrogen atoms were refined anisotropically by full-matrix least-squares (SHELXL-97).[9] All hydrogen atoms were placed using a riding model, and their positions constrained relative to their parent atom using the appropriate HFIX command in SHELXL-97.

Structure of 3. 3 was isolated from the dissolution of $CoCl_2$ in MeCN, and determination of its unit cell parameters [a = 8.904 Å, b = 8.400 Å, c = 24.102 Å, β = 93.42°] was in accord with that reported for $[Co^{II}(NCMe)_6][Co^{II}Cl_3(NCMe)]_2 \cdot MeCN$.[13]

Structure of 4. 4 was isolated in an unexpected reaction as discussed in the text (vide infra). A blue-colored crystal was mounted on a CryoLoop with Paratone-N oil. Data were collected on a Bruker SMART APEX CCD diffractometer using Mo K_α radiation. Data were corrected for adsorption with SADABS, and the structure was solved using a Patterson Synthesis and refined by full-matrix, least-squares on F^2, and all non-hydrogen atoms were refined anisotropically. Hydrogen atoms were placed in calculated positions relative to their parent C atoms with fixed U values of −1.2 and −1.5. The hydrogen atoms on C2 were found from a Fourier difference map and were fixed in their positions. Carbon atoms C4 and C10 of the NEt_4^+ counterion exhibited large thermal parameters, but the disorder was not treated. Despite the β angle being almost exactly 90°, diffraction symmetry indicated that no symmetry higher than monoclinic existed. A pseudo-merohedral twin refinement was used in the final steps of analysis and indicated a 50:50 twin ratio.

Results and Discussion

Several anionic and neutral chloroiron(II) and (III) species are known to exist in equilibrium with each other, both in aqueous and in nonaqueous solutions,[14] but not acetonitrile. This is in contrast to iodoiron(II) and (III) species whose chemistry in MeCN,[15] as well as that of the Co(II) chlorides,[16] has been described.

Slow diffusion of Et_2O into a saturated MeCN solution of MCl_2 (MMn, Fe) forms colorless, prism-shape crystals of $MCl_2(NCMe)_2$ [M = Fe (**1**), Mn (**2**)] composition. However, dissolution of $CoCl_2$ in MeCN forms deep blue crystals of $[Co^{II}(NCMe)_6][Co^{II}Cl_3(NCMe)]_2 \cdot MeCN$ (**3**) composition. Whereas $[NEt_4]_2[Co^{II}Cl_4]$ can be prepared from ethanol, from MeCN it is isolated as the $[Co^{II}Cl_3(NCMe)]^-$ anion.[17]

Thermal Properties. The TGA of **1** revealed two almost identical weight loss steps (∼17%) with maximal rates at 84 and 146 °C (Figure 1), which are observed in DSC scans as two irreversible endothermic events with ΔH = 44.3 and 54.8 kJ/mol, respectively. These weight loss magnitudes correspond to two sequential losses of MeCN: $Fe^{II}Cl_2(NCMe)_2 \rightarrow Fe^{II}Cl_2(NCMe) \rightarrow Fe^{II}Cl_2$. A similar effect was observed for **2** with 18.6% weight loss at 93 °C. Likewise, $Fe^{II}Cl_2py_4$ (py = pyridine) exhibits a similar thermal decomposition to $Fe^{II}Cl_2py_2$ and $Fe^{II}Cl_2py$.[18]

Structures. The structure of **1** (Figure 2) (and isostructural **2**) contains polymeric 1-D chains consisting of octahedrally

(12) TOPAS-Academic is available at http://pws.prserv.net/Alan.Coelho.
(13) Malkov, A. E.; Fomina, I. G.; Sidorov, A. A.; Aleksandrov, G. G.; Egorov, I. M; Latosh, N. I.; Chupakhin, O. N.; Rusinov, G. L.; Rakitin, Yu. V.; Novotortsev, V. M.; Ikorskii, V. N.; Eremenko, I. L.; Moiseev, I. I. *J. Mol. Struct.* **2003**, *656*, 207. CCDB Code JOYPUI01.
(14) (a) See, e.g. Cotton, F. A.; Wilkinson, G. In *Advanced Inorganic Chemistry*, 5th ed.; Wiley: New York, 1988; p 718. (b) Rollick, K. L.; Kochi, J. K. *Organometallics* **1982**, *1*, 725, and references therein. (c) Brenner, L. S.; Root, C. A. *Inorg. Chem.* **1972**, *11*, 652. (d) Work, R. A., III; McDonald, R. L. *Inorg. Chem.* **1973**, *12*, 1936. (e) Long, G. L.; Whitney, D. L.; Kennedy, J. E. *Inorg. Chem.* **1971**, *10*, 1406.
(15) Pohl, S.; Saak, W. *Z. Naturforsch.* **1984**, *39b*, 1236.
(16) Libus, W. *Rocz. Chem.* **1962**, *36*, 999.
(17) Gill, N. S.; Taylor, F. B. *Inorg. Synth.* **1967**, *9*, 139.
(18) Taminaga T.; Takeda M.; Marimoto T.; Saito N. *Bull. Chem. Soc. Jpn.* **1970**, 1093.

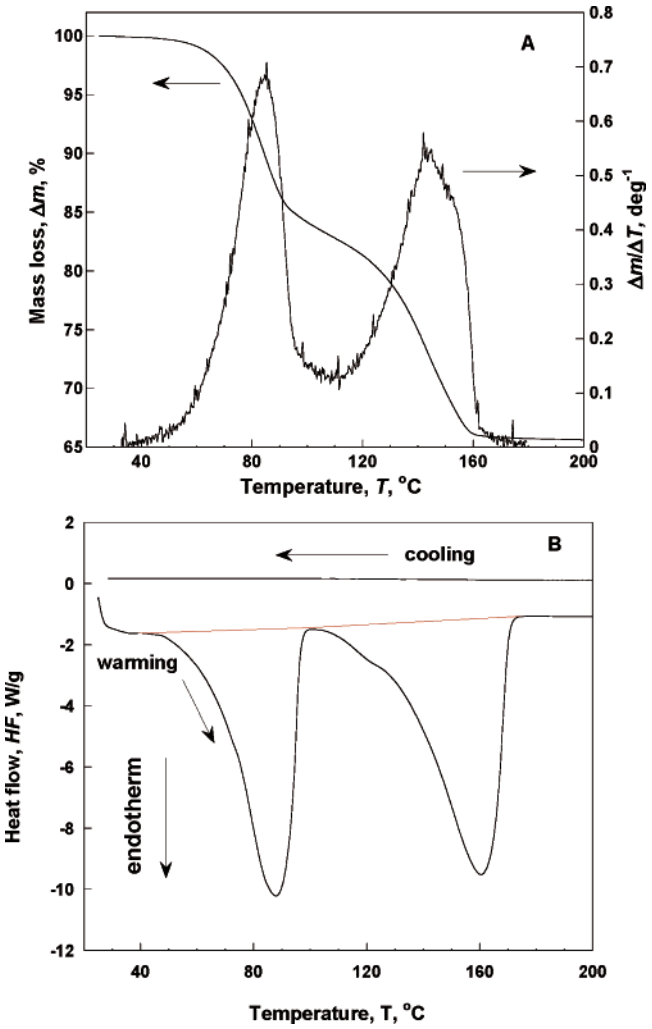

Figure 1. TGA (A) and DSC (B) traces in the $20 \leq T \leq 200$ °C region for $FeCl_2(MeCN)_2$. Analysis was performed assuming a linear background.

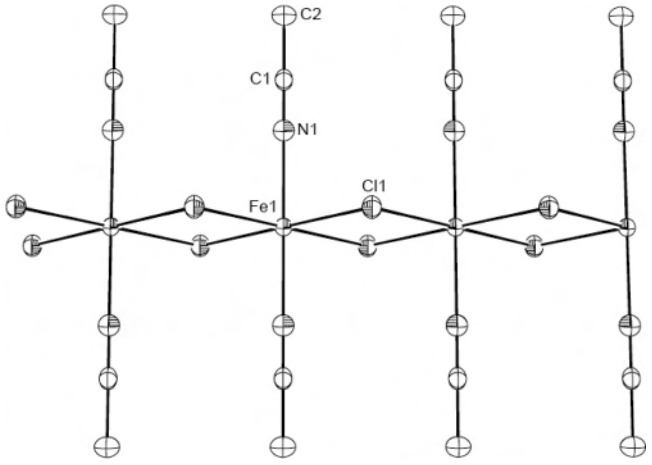

Figure 2. ORTEP atom labeling diagram of **1**; **2** is isostructural. Fe−Cl = 2.5006(3) Å, Fe−N = 2.1591(14) Å, Mn−Cl = 2.5396(7) Å, and Mn−N = 2.2426(18) Å.

coordinated Fe^{II} ions symmetrically bridged by four chloride ligands with Fe−Cl and Mn−Cl distances of 2.5006(3) and 2.5396(7) Å, respectively, and average Cl−M−Cl angles of 84.5° (MFe) and 85.06° (MMn), respectively. Two apical octahedral positions are occupied with MeCN molecules with average Fe−N and Mn−N distances 2.159 and 2.243 Å, respectively. While the M−Cl distances are comparable to each other, the Mn−N distance is 0.084 Å longer, suggestive of the expected Jahn−Teller contractive distortion for Fe(II). The Me Hs groups exhibit a 50:50 orientation disorder due to an imposed crystallographic symmetry. Similar 1-D chain structural motifs were observed for the pyridine (py) complexes containing first-row M^{II} chlorides of $M^{II}py_2Cl_2$ (MFe;[19a] Co;[19b] Mn;[19c] Cu[19d]) composition. In these compounds, average M−Cl distances and Cl−M−Cl angles are in the range of 2.6 ± 0.1 Å and 86 ± 2°, respectively, in accord with our observations.

The loss of MeCN via two distinct steps (Figure 1) suggests that the unknown monosolvate, $Fe^{II}Cl_2(NCMe)$, might be isolated. Annealing **1** at 55 ± 5 °C for 2 h leads to formation a **1a**. The powder X-ray diffraction (XRD) pattern for **1a** indicates a pure phase is formed that lacks **1**. The structure of **1a** was determined with the Rietveld analysis of the synchrotron powder diffraction data based upon the chemical composition. The Rietveld refinement is shown in Figure 3, and selected diffraction data are given in Table 1.

The structure of **1a** contains polymeric 1-D chains consisting of octahedrally coordinated Fe^{II} ions symmetrically bridged by four chloride ligands with average μ-Fe−Cl and μ_3-Fe−Cl distances of 2.451 (6) and 2.548 (6) Å, respectively, and an Fe−N distance of 2.143 (8) Å (Figure 4). The Fe−N−C angle of 165.3(43)° deviates significantly from linearity, as has been observed for other structures.[20]

The chains are shifted with respect to another by *c*/2 along the chain (*c*) axis such that every second Cl from one chain is coordinated to the apical octahedral position of the Fe of the other chain. Thus, each Fe is coordinated to five chlorides and one MeCN in the remaining apical octahedral position. This transformation presumably occurs when the two closest Fe atoms from adjacent chains of **1** lose the MeCN oriented toward the neighboring chain, and the chains can collapse or condense into a double chain with formation of Fe−Cl bonding such that half of the μ-Cl's become μ_3-Cl's (see TOC illustration). The endothermic character of the transformation is consistent with Fe−N bond breaking.

In contrast, the structures of **3** and **4** possess tetrahedral $[Co^{II}Cl_3(NCMe)]^-$ anions, with **3** and **4** having the $[Co^{II}(NCMe)_6]^{2+}$ and $[NEt_4]^+$ cations, respectively. The structure of **3** exists in the Cambridge Crystal data base,[13] with an average Co−N distance of 2.114 Å within the $[Co^{II}(NCMe)_6]^{2+}$ ion that is identical to that observed for $[Co^{II}(NCMe)_6](SbF_6)_2$ (2.111 Å).[21a] $[NEt_4][Co^{II}Cl_3(NCMe)]$ (Figure 5) was unexpectedly isolated as a byproduct from the

(19) (a) Long, G. J.; Whitney, D. L.; Kennedy, J. E. *Inorg. Chem.* **1971**, *10*, 1406. (b) Dunitz J. D. *Acta Crystallogr.* **1957**, *10*, *307*. (c) Richards, P. M.; Quinn, R. K.; Morosin. *B. J. Chem. Phys.* **1973**, *59*, 4474. (d) Takeda K.; Matsukawa S.; Haseda T. J. *Phys. Soc. Jpn.* **1971**, *30*, 1330.
(20) See, for example, Cambridge Database structures AEFGIB, AVINUO, MOPSIT, TUJHIP.
(21) (a) Rheingold, A. L. Giles, I.; Miller, J. S. Unpublished results. (b) Kennon, B. S.; Miller, J. S. Unpublished results.

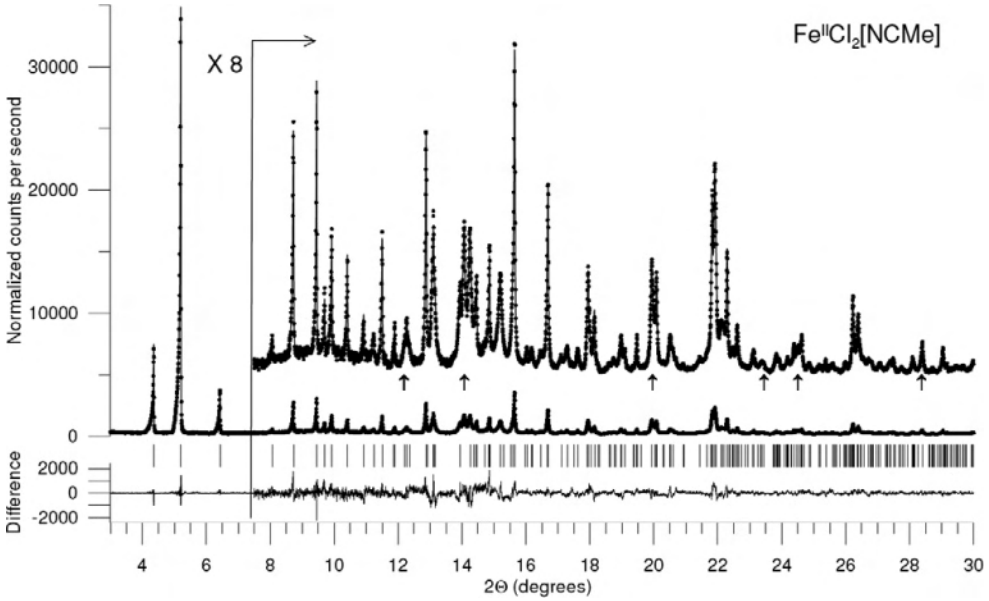

Figure 3. XRD pattern for **1a** at room temperature and Rietveld fit to the Synchrotron powder diffraction data structure of **1a** that includes 7% NaCl impurity (peak position indicated by arrows). In the upper trace, data points are denoted by filled circles, the best Rietveld fit by a smooth curve. The vertical tick marks indicate positions of allowed Bragg peaks. The lower trace is the difference between the observed and calculated data on the same vertical scale.

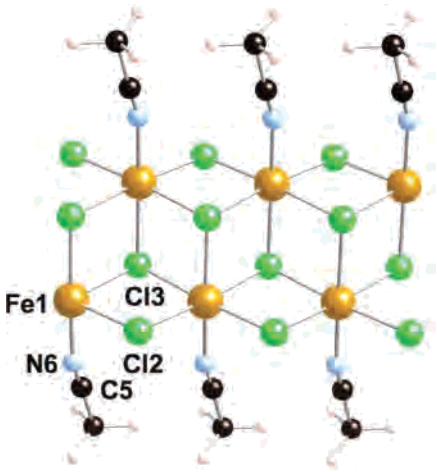

Figure 4. Atom labeling diagram of **1a**. Fe1−Cl2 = 2.443(4) and 2.459-(4) [average = 2.451(6) Å], Fe1−Cl3 = 2.533(4), 2.544(3), and 2.566(4) [average = 2.548(6) Å], Fe1−N6 = 2.143(8) Å.

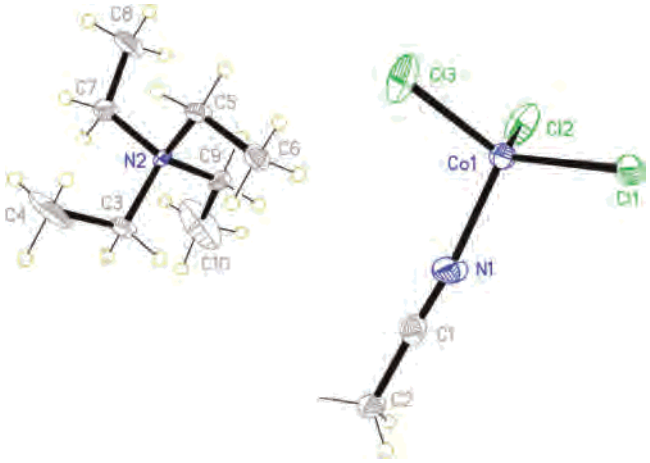

Figure 5. Atom labeling diagram of **4**. Co1−Cl1 = 2.230(1) Å, Co1−Cl2 = 2.247(4), Co1−Cl3 = 2.229(4) Å, and Co1−N1 = 2.012(4).

reaction of $[NEt_4][Ru_2(O_2CMe)_4Cl_2]$[22] and $[Co^{II}(NCMe)_6](BF_4)_2$.[21b] The $[CoCl_3(NCMe)]^-$ anions for **3** and **4** are structurally identical, with average Co−N and Co−Cl distances of 2.032 and 2.269 Å, respectively.

IR Spectra. As expected, the mid-IR spectra of **1**, **2**, and **1a** are essentially identical and consist of MeCN vibrations ($\nu_{CN} = 2282 \pm 2$ cm^{-1}) in accord with previously reported values,[23] with the aliphatic ν_{CH} stretching modes at 2992 and 2933 cm^{-1} for **1** shift to 3002 and 2939 cm^{-1} for **1a**. However, the broad (due to the CH_3 group rotation) band at 1420 cm^{-1} in **1** in the region of asymmetric CH_3 modes resolves into four peaks at 1405, 1418, 1431, and 1444 cm^{-1} characteristic for solid MeCN at 77 K, implying that the CH_3 position in **1a** is locked. In addition, the symmetric deformation mode at 1378 cm^{-1} for **1** shifts to 1365 cm^{-1} for **1a**.

In the far-IR region, the Fe−N stretching mode[24] was observed at 396 cm^{-1} for **1** and **1a**. Two peaks in **1** at 234 and 194 cm^{-1} were assigned to Fe−Cl stretching modes, and the peaks at 152 and 63 cm^{-1} to Cl−Fe−Cl deformation vibrations following the assignment of similar vibration in the $[Fe^{II}Cl_4]^{2-}$ ion.[25] In **1a**, 194 and 152 cm^{-1} peaks shift to 182 and 147 cm^{-1}, respectively, and no new peaks appear, implying that the local distorted octahedral geometry remains intact.

Magnetic Properties. The 5−300-K temperature-dependent magnetic susceptibility, χ, of **1**, **1a**, **2**, **3**, and **4** are

(22) Barral, M. C.; Gonzalez-Prieto, R.; Herrero, S.; Jimenez-Aparicio, R.; Priego, J. L.; Torres, M. R.; Urbanos, F. A. *Polyhedron* **2005**, *24*, 239.
(23) Pace, E. L.; Noe, L. J. *J. Chem. Phys.* **1968**, *49*, 5317.
(24) Nakamoto, K. In *Infrared and Raman spectra of Inorganic and Coordination Compounds Part B: Application in Coordination, Organometallic and Bioinorganic Chemistry*, 5th ed.; Wiley-Interscience: New York, 1997; p 113.
(25) Sabatini, A.; Sacconi, l. *J. Am. Chem. Soc.* **1964**, *86*, 17.

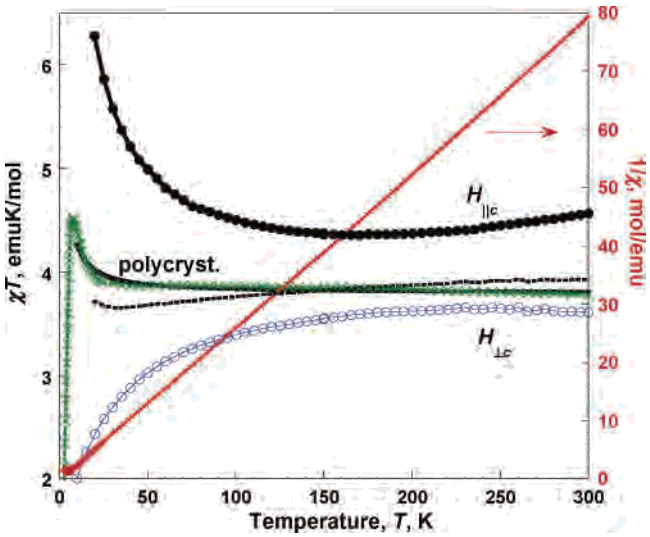

Figure 6. $\chi T(T)$ (×) and $\chi^{-1}(T)$ (+) for polycrystalline powder of (**1**) with $\chi T(300\ \mathrm{K}) = 3.8$ emuK/mol, $\theta = 1.1$ K fitted to the Curie−Weiss law, solid line. $\chi T(T)$ for crystal mosaic aligned with $H_{\parallel c}$ (●) and $H_{\perp c}$ (○). Dotted line is $\chi_{av}T(T) = (\chi_{\parallel}T + 2\chi_{\perp}T)/3$.

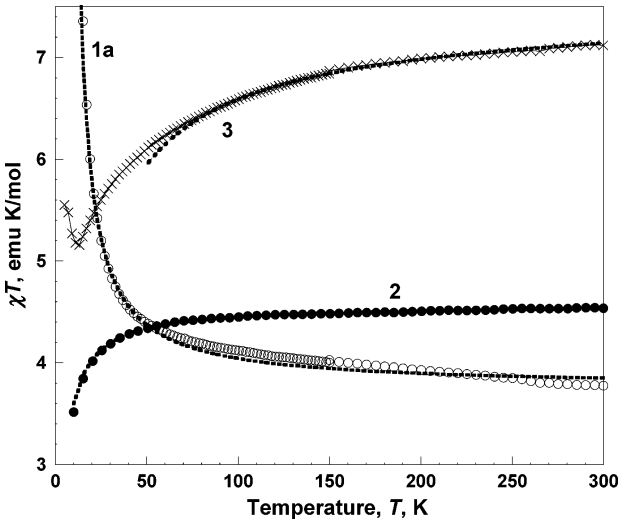

Figure 7. $\chi T(T)$ for polycrystalline sample of **1a** (○), **2** (●), and **3** (×). Dotted lines are their fit to Curie−Weiss law with $\chi T(300\ \mathrm{K}) = 3.77$ emuK/mol, $\theta = 7.0$ K; $\chi T(300\ \mathrm{K}) = 4.55$ emuK/mol, $\theta = -2.7$ K; and $\chi T(300\ \mathrm{K}) = 7.1$ emuK/mol, $\theta = -12$ K, respectively.

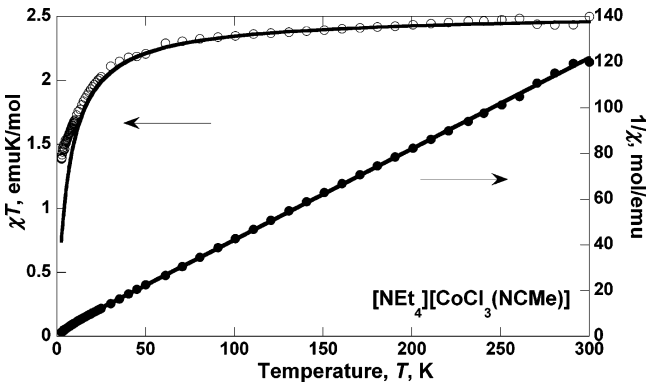

Figure 8. Observed $\chi T(T)$ and $\chi^{-1}(T)$ for **4**. Solid lines are fits to Curie−Weiss law with $g = 2.30$, $\theta = -6.2$ K, and TIP $= 10^4$ emu/mol.

reported as $\chi T(T)$, Figures 6−8. The value of χT at 300 K for **1** is 3.78 emuK/mol, which is slightly lower than expected for high-spin octahedral Fe(II) with weak spin−orbit coupling (3.98 emuK/mol),[26] as occurs due to a departure from ideal octahedral symmetry. This value is close to that obtained for $FeCl_2(py)_2$ (3.66 emuK/mol).[27] The presence of an axial distortion causes a significant anisotropy of χ with respect to magnetic field, H, being parallel or perpendicular to the c axis (Figure 6), which is parallel to the Fe−Cl chain direction. On cooling the anisotropy increases significantly below 150 K; however, both $\chi_{\parallel}$ and $\chi_{\perp}$ separate in such a way that the average value χ_{av} $[=(\chi_{\parallel} + 2\chi_{\perp})/3]$ almost coincides with the average powder value. Being almost temperature independent down to 25 K, $\chi T(T)$ increases to 4.5 emuK/mol at 8 K and then drops abruptly, implying an antiferromagnetic ground state. However, $\chi T(T)$ does not vanish at 2 K, indicating that it may occur substantially below 2 K. Above 25 K, $\chi^{-1}(T)$ can be fit to the Curie−Weiss expression $[\chi \propto (T - \theta)^{1/2}]$ with $\theta = 1.1$ K, which is in accord with the theory predicting ferromagnetic superexchange through Fe−Cl−Fe bridges, since they all are lying in the same plane, and Cl−Fe−Cl angles do not differ greatly from 90°.[28] At low temperatures, antiferromagnetic interchain interactions prevail (most probably due to a lattice contraction), and the system undergoes a transition to an antiferromagnetic state below 2 K.

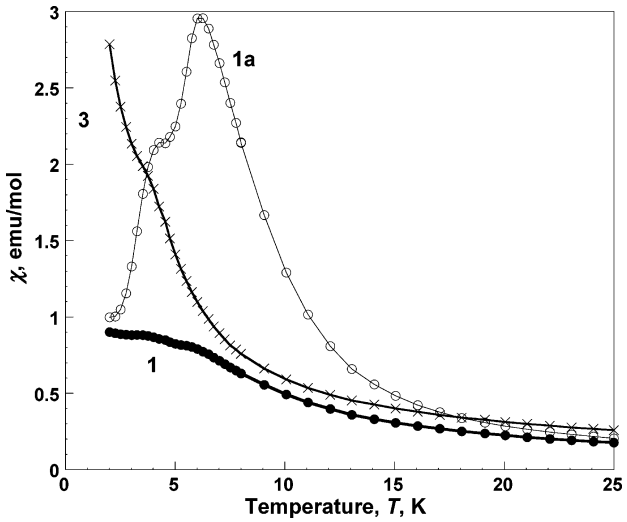

Figure 9. $\chi(T)$ for polycrystalline samples of **1** (●), **1a** (○), and **3** (×).

The 5−300-K $\chi T(T)$ of **2** and **3** is shown in Figure 7. The $\chi T(300\ \mathrm{K})$ of 4.54 emuK/mol for **2** is in accord with the expected value for high-spin Mn(II) (4.375 emuK/mol),[26b] and negative $\theta = -2.7$ K implies an antiferromagnetically

(26) Casey, A. T.; Mitra, S. Magnetic Behavior of Compounds Containing d^n Ions. In *Theory and Application of Molecular Paramagnetism*; Boudreaux, E. A., Mulay, L. N., Eds.; John Wiley and Sons: New York, 1976. The reported range (a) for high-spin Fe(II) is $3.37 \le \chi T \le 3.85$ (p 200); (b) for Mn(II) $3.25 \le \chi T \le 4.41$ (p 185); for Co(II) $2.42 \le \chi T \le 3.39$ (p 214).

(27) Long, G. J.; Whitney, D. L.; Kennedy, J. E. *Inorg. Chem.* **1971**, *10*, 1406.

(28) Anderson, P. W. *Phys. Rev.* **1950**, *79*, 350. Anderson P. W. *Phys. Rev.* **1959**, *115*, 2. Anderson P. W. Exchange in Insulators: Superexchange, Direct Exchange, and Double Exchange. In *Magnetism, I*; Rado, G. T., Shuhl H., Eds.; Academic Press: New York, 1963; p 67. Goodenough, J. B. *Phys. Chem. Solids* **1958**, *6*, *287*. Goodenough, J. B. *Phys. Rev.* **1955**, *100*, 504. Kanamori, J. *Phys. Chem. Solids* **1959**, *10*, 87.

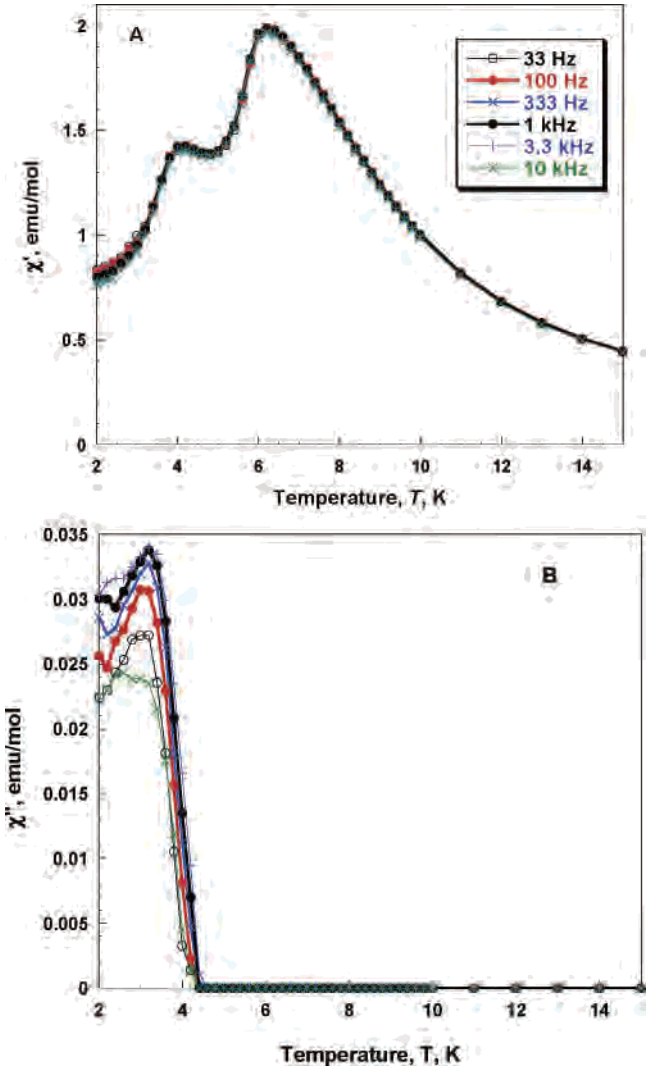

Figure 10. $\chi'(T)$ (a) and $\chi''(T)$ (b) for polycrystalline sample of **1a** at different frequencies.

coupled ground state. Similar to **1**, $\chi(T)$ does not vanish at 2 K, suggesting $T_c < 2$ K. The χT(300 K) of 7.15 emuK/mol for **3** is lower than the expected value for three high-spin Co(II) ions;[26c] however, a negative $\theta = -12$ K implies significant antiferromagnetic coupling which suppresses χT even at room temperature.

The room-temperature χT value for **4** is 2.50 emuK/mol, which is larger that the expected spin-only values of 1.875 emuK/mol for an $S = 3/2$ system. This deviation of the spin-only value is expected for Co(II) due to its anisotropic g value. The $\chi T(T)$ decreases with decreasing temperature, and the data can be fit to the Curie−Weiss expression for $S = 3/2$ with $g = 2.30$, $\theta = -6.2$ K, and TIP $= 10^4$ emu/mol (Figure 8). Similar to **3** this indicates antiferromagnetic coupling between Co(II) sites.

The magnetic behavior of **1a** is very different. At room temperature, χT(300 K) is 3.78 emuK/mol, which is similar to that for **1**; the fit of $\chi T(T)$ to the Curie−Weiss expression reveals a positive θ of 7.1 K. Below 20 K, $\chi T(T)$ rapidly increases with decreasing temperature, indicating a magnetic transition. The low-temperature behavior of $\chi(T)$ is more complex (Figure 9). It reaches a maximum at 6.1 K and then decreases down to 4.6 K on further cooling. Below 4.6 K it increases slightly again, reaches another maximum at 4.3 K, and then decreases to ~1 emu/mol at 2 K. It should be noted that no irreversibility was observed between zero-field-cooled and field-cooled $\chi(T)$. These two transitions also reveal themselves as two more resolved peaks at 6.25 and 4.15 K in the in-phase $\chi'(T)$ component of the ac susceptibility (33−10 000 Hz frequency range) (Figure 10a). The peaks positions are frequency independent, which together with the lack of irreversibility below the transition temperature suggests good sample crystallinity. The out-of-phase component of the ac susceptibility, $\chi''(T)$ (Figure 10b), appears only below the second transition at 4.2 K. A similar effect was observed for $Fe[TCNE]_2$[29,30] where a parallel and perpendicular to magnetic field component of magnetization ordered at different temperatures. Here 3-D magnetic ordering is achieved below 4.3 K where the nonvanishing $\chi''(T)$ starts to be observed.

The shape of field dependence of magnetization, $M(H)$, of **1** at 2 K is, as expected, for a paramagnet. The $M(H)$ at 5 T is 15 100 emu·Oe/mol and is in a good agreement with 14 500 emu·Oe/mol reported for $FeCl_2(py)_2$.[31] However, the 9-T high-field value is substantially suppressed (~60% of the expected value calculated via Brillouin function for $S = 2$ and $g = 2.25$) in accord with its antiferromagnetic behavior at low temperatures. In contrast, $M(H)$ of **1a** increased rapidly with the field attaining about half of its expected saturated magnetization value at 6000 Oe. Upon further increasing the field, $M(H)$ approached a saturation value at a much slower rate and saturation was not achieved at 9 T. This is most probably due to an enormous magnetic anisotropy of this compound at low temperature. However, more detailed studies of this effect are needed.

Acknowledgment. The continued partial support by the Department of Energy Division of Materials Science (Grants No. DE-FG03-93ER45504, DE FG 02-86BR45271, and DE-FG02-01ER45931) and the Air Force Office of Scientific Research (F49620-03-1-0175) is appreciated. Use of the National Synchrotron Light Source, Brookhaven National Laboratory, was supported by the U.S. Department of Energy, Office of Basic Energy Sciences, under Contract No. DE-AC02-98CH10886.

Supporting Information Available: X-ray crystallographic data for **1** (CCDC no. 622332), **1a** (CCDC no. 622330), **2** (CCDC no. 622331), and **4** (CCDC no. 622333) in CIF format. This material is available free of charge via the Internet at http://pubs.acs.org.

IC061877N

(29) Pokhodnya, K. I.; Petersen, N.; Miller, J. S. *Inorg. Chem.* **2002**, *41*, 1996.
(30) Gírtu, M. A.; Wynn, C. M.; Zhang, J.; Miller, J. S.; Epstein, A. J. *Phys. Rev.* **2000**, *B61*, 492.
(31) Foner, S.; Frankel, R. B.; Reiff, W. M.; Little, B. F.; Long, G. J. *Solid State Commun.* **1975**, *16*, 159.